2011 American Control Conference
on O'Farrell Street, San Francisco, CA, USA
June 29 - July 01, 2011

Discretization Methods for Battery Systems Modeling

Ying Shi, Githin Prasad, Zheng Shen and Christopher D. Rahn

Abstract— **First principles battery models, consisting of nonlinear coupled partial differential equations, are often difficult to discretize and reduce in order so that they can be used by systems engineers for design, estimation, prediction, and management. In this paper, six methods are used to discretize a benchmark electrolyte diffusion problem and their time and frequency response accuracy is determined as a function of discretization order. The Analytical Method (AM), Integral Method Approximation (IMA), Padé Approximation Method (PAM), Finite Element Method (FEM), Finite Difference Method (FDM) and Ritz Method (RM) are formulated for the benchmark problem and convergence speed and accuracy calculated. The PAM is the most efficient, producing 99.5% accurate results with only a 3rd order approximation. IMA, Ritz, AM, FEM, and FDM required 4, 6, 9, 14, and 27th order approximations, respectively, to achieve the same error.**

Index Terms— **Numerical methods, diffusion equations, convergence.**

I. INTRODUCTION

A variety of electrochemical power sources such as lead-acid, lithium ion, nickel-cadmium (Ni-Cd) and nickel-metal hydride (Ni-MH) batteries as well as fuel cells, are widely used in industrial applications (e.g. UPS and power plants) and hybrid electric vehicles/locomotives. These applications demand sophisticated design and control to provide high energy/power density and long cycle life. Accurate mathematical models are crucial for optimal energy storage system design and real-time estimation, prediction, and control. First principles models have been developed for lead-acid batteries [1], [2], [3], NiCd/NiMh batteries [4], [5], [6], lithium-ion batteries [7], [8], [9] and fuel cells [10], [11]. These models can accurately predict the system performance once the nonlinear and coupled partial differential differential equations (PDEs) that comprise the model are solved numerically using, for example, the control-volume method [5]. Other researchers propose equivalent circuit models [12], [13] but the model parameters lack physical meaning and connection to the underlying the electrochemical processes. In this paper, several discretization techniques are investigated to convert the PDEs of diffusion-type processes like batteries and fuel cells into a set of ODEs. This approach maintains the connection with the fundamental electrochemical governing equations. System order is the critical factor for fast computation and real-time implementation so the convergence and accuracy of the different techniques as a function of the number of integrators in the model is studied.

This work was supported by Norfolk Southern and DOE

Christopher D. Rahn is with the Department of Mechanical and Nuclear Engineering, The Pennsylvania State University, University Park, PA 16802, USA, cdrahn@engr.psu.edu

To compare the various discretization techniques, the benchmark problem shown in Fig. 1 is proposed and used throughout the work. The electrolyte phase diffusion problem for a battery cell with uniform reaction current distribution and two coupled domains includes many of the key features of battery cell models, including diffusion dynamics and spatially varying inputs and parameters. The two domains correspond to a porous negative electrode ($0 < x < L/2$) and a porous positive electrode ($L/2 < x < L$). For simplicity, the two electrodes are assumed to be the same length ($L/2$) and that the diffusion coefficients and electrode phase volume fractions are different for (but constant within) the two electrodes. The current density $j(t) = 2I(t)/(AL)$ for the negative electrode and $j(t) = -2I(t)/(AL)$ for the positive electrode where A is the electrode plate area and $I(t)$ is the total current flowing through the cell. Thus, the coupled domains model consists of the two field equations

$$\begin{aligned} \varepsilon_m \frac{\partial c}{\partial t} &= D_m \frac{\partial^2 c}{\partial x^2} + b\,I \quad \text{for } x \in (0, L/2), \\ \varepsilon_p \frac{\partial c}{\partial t} &= D_p \frac{\partial^2 c}{\partial x^2} - b\,I \quad \text{for } x \in (L/2, L), \end{aligned} \tag{1}$$

where $c(x,t)$ is the ion concentration and ε_m and ε_p and D_m and D_p are the electrode phase volume fractions and diffusion coefficients for the negative and positive electrode, respectively. The diffusion coefficients depend on a reference diffusion coefficient D^{ref} and the phase volume fractions as follows:

$$D_m = D^{ref}\varepsilon_m^{1.5} \text{ and } D_p = D^{ref}\varepsilon_p^{1.5},$$

The input constant

$$b = \frac{2(1-t_0)}{FAL}, \tag{2}$$

where t_0 is the transference number and F is Faraday's constant. Ions do not flux through the boundaries so the boundary conditions

$$\left.\frac{\partial c}{\partial x}\right|_{x=0} = \left.\frac{\partial c}{\partial x}\right|_{x=L} = 0, \tag{3}$$

$$\begin{aligned} D_m \left.\frac{\partial c}{\partial x}\right|_{x=(L/2)_-} &= D_p \left.\frac{\partial c}{\partial x}\right|_{x=(L/2)_+}, \\ c\left(\frac{L}{2_-}, t\right) &= c\left(\frac{L}{2_+}, t\right), \end{aligned} \tag{4}$$

At the interface between the two domains, the boundary conditions Eq. (4) couple the two domains by ensuring continuity of concentration and flux through the boundary at $x = L/2$. In this problem, the output is taken to be

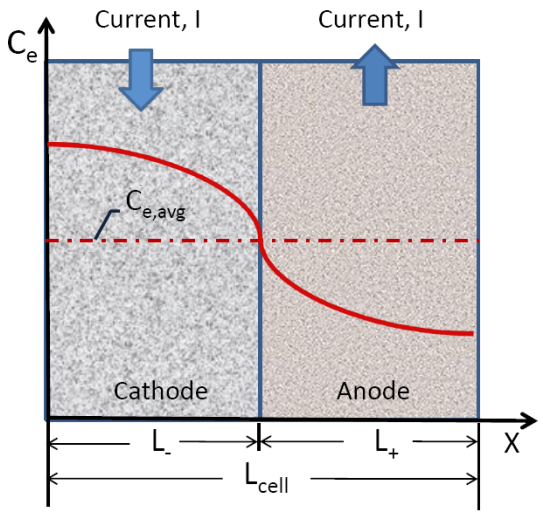

Fig. 1. Schematic diagram of the benchmark electrolyte diffusion problem

$y(t) = c(L,t) - c(0,t)$ because the output voltage for a cell typically depends on the concentration difference between the two electrodes.

II. Discretization Methods

A. Analytical Method (AM)

Most of the PDEs that are encountered in battery systems are approximately linear with constant coefficients so we can often find an exact or analytical solution. In this section, we exactly solve the benchmark electrolyte diffusion problems. More information on analytical methods can be found in [14], [15], [16], [17].

Two approaches are used to analytically/exactly solve the benchmark problem. First, we use the separation of variables to generate an eigenvalue problem that is then solved. The spatially distributed response is calculated from a eigenfunction series expansion. If the eigenfunction expansion is truncated then the resulting model can be put in state variable form, allowing time and frequency response calculations. Second, we use the Laplace transform to eliminate time derivatives and solve the resulting ordinary differential equations for a transcendental transfer function. This allows calculation of the exact frequency response without truncation of the eigenfunction series but the transcendental transfer function cannot be directly used for time simulation.

Eigenfunction Expansion: The eigenvalue problem is derived by substituting $c(x,t) = C(x)e^{\lambda t}$ into Eqs. (1) with $I(t) = 0$ to produce

$$\begin{aligned} \varepsilon_m \lambda C_m - D_m C_m'' &= 0 \quad \text{for } x \in (0, L/2), \\ \varepsilon_p \lambda C_p - D_p C_p'' &= 0 \quad \text{for } x \in (L/2, L). \end{aligned} \tag{5}$$

The solutions of Eqs. (5) are

$$\begin{aligned} C_m(x) &= C_{1m} e^{\beta_m x} + C_{2m} e^{-\beta_m x}, \\ C_p(x) &= C_{1p} e^{\beta_p x} + C_{2p} e^{-\beta_p x}. \end{aligned} \tag{6}$$

Substitution of Eqs. (6) into Eqs. (5) produces

$$\lambda = \frac{D_m \beta_m^2}{\varepsilon_m} = \frac{D_p \beta_p^2}{\varepsilon_p} \tag{7}$$

or

$$\beta_m = \alpha \beta_p, \ \varepsilon_m = \zeta \varepsilon_p, \text{ and } D_m = \frac{\zeta D_p}{\alpha^2} \tag{8}$$

where

$$\alpha = \sqrt{\frac{D_p \varepsilon_m}{D_m \varepsilon_p}} \text{ and } \zeta = \frac{\varepsilon_m}{\varepsilon_p} \tag{9}$$

Substitution of Eq. (7) into the solutions Eqs. (6) and then into the boundary conditions Eqs. (3) and (4) produces the matrix equation

$$\mathbf{M}\mathbf{c} = \mathbf{0}, \tag{10}$$

where $\mathbf{c} = [C_{1m}, C_{2m}, C_{1p}, C_{2p}]^T$ and

$$\mathbf{M} = \begin{bmatrix} \alpha\beta_p & -\alpha\beta_p & 0 & 0 \\ \alpha\zeta\beta_p e^{\frac{1}{2}\alpha\beta_p L} & -\alpha\zeta\beta_p e^{-\frac{1}{2}\alpha\beta_p L} & -\alpha^2\beta_p e^{\frac{1}{2}\beta_p L} & \alpha^2\beta_p e^{-\frac{1}{2}\beta_p L} \\ e^{\frac{1}{2}\alpha\beta_p L} & e^{-\frac{1}{2}\alpha\beta_p L} & -e^{\frac{1}{2}\beta_p L} & -e^{-\frac{1}{2}\beta_p L} \\ 0 & 0 & \beta_p e^{\beta_p L} & -\beta_p e^{-\beta_p L} \end{bmatrix}. \tag{11}$$

Eq. (11) has nonzero solutions if the determination of $\mathbf{M}$ satisfies

$$\begin{aligned} |\mathbf{M}| = -\alpha^2\beta_p^3 \Big[&(\zeta - \alpha)\left(e^{-\beta_p \gamma_1} - e^{\beta_p \gamma_1}\right) \\ &+ (\zeta + \alpha)\left(e^{-\beta_p \gamma_2} - e^{\beta_p \gamma_2}\right)\Big] = 0 \end{aligned} \tag{12}$$

where $\gamma_1 = L(\alpha - 1)/2$ and $\gamma_2 = L(\alpha + 1)/2$. Note that the eigenvalue problem in Eq. (12) reduces to

$$e^{\beta L} - e^{-\beta L} = 0, \tag{13}$$

if $\alpha = 1$ and $\zeta = 1$ because this is corresponds to the single domain problem with $D_p = D_m$ and $\varepsilon_p = \varepsilon_m$. Eq. (12) can also be written using hyperbolic functions as

$$\beta_p{}^3 \left[(\zeta - \alpha)\sinh(\beta_p \gamma_1) + (\zeta + \alpha)\sinh(\beta_p \gamma_2)\right] = 0 \tag{14}$$

Eq. (12) has only imaginary roots $\beta_p = \sqrt{\varepsilon_p \lambda / D_p}$ corresponding to real and negative eigenvalues $\lambda < 0$. These roots are found numerically and substituted into Eq. (11), making $\mathbf{M}$ singular. The eigenvector corresponding to the zero eigenvalue provides the eigenfunction coefficients $C_{1m}, \ldots, C_{2p}$. These eigenfunctions are orthogonal. The elements of the $\mathbf{B}$ vector are

$$b_n = \int_0^{L/2} b\, C_n(x)\, dx - \int_{L/2}^{L} b\, Cn(x)\, dx. \tag{15}$$

The output is expressed as an eigenfunction series evaluated at $x = L$ minus $x = 0$.

Transfer Function: Laplace transform of Eqs. (1) produces

$$\begin{aligned} s\varepsilon_m C_m - D_m C_m'' - b\, I &= 0 \quad \text{for } x \in (0, L/2), \\ s\varepsilon_p C_p - D_p C_p'' + b\, I &= 0 \quad \text{for } x \in (L/2, L). \end{aligned} \tag{16}$$

The solutions of Eqs. (16) are

$$\begin{aligned} C_m(x) &= C_{1m} e^{\beta_m x} + C_{2m} e^{-\beta_m x} + \frac{b\, I}{\varepsilon_m s}, \\ C_p(x) &= C_{1p} e^{\beta_p x} + C_{2p} e^{-\beta_p x} - \frac{b\, I}{\varepsilon_p s}. \end{aligned} \tag{17}$$

Substitution of Eqs. (17) into Eqs. (16) produces

$$s = \frac{D_m \beta_m^2}{\varepsilon_m} = \frac{D_p \beta_p^2}{\varepsilon_p} \tag{18}$$

and the same relationships in Eq. (8) and (9). Substitution of Eq. (18) into the solutions (17) and then into the boundary conditions Eqs. (3) and (4) produces four linear equations in four unknowns $C_{1m},\ldots,C_{2p}$. The transfer function

$$\frac{D_p Y(s)}{b\,\varepsilon_p I(s)} = \frac{\begin{array}{c} 4\,\alpha \sinh\left(\frac{1}{2}\beta_p L\right) - 2\,(\zeta-\alpha)\sinh(\beta_p \gamma_1) \\ +\,4\,\zeta \sinh\left(\frac{1}{2}\alpha\,\beta_p L\right) - 2\,(\zeta+\alpha)\sinh(\beta_p \gamma_2) \end{array}}{{\beta_p}^2\left[(\zeta-\alpha)\sinh(\beta_p \gamma_1) + (\zeta+\alpha)\sinh(\beta_p \gamma_2)\right]} \tag{19}$$

results from substituting these solutions into $Y(s) = C(L,s) - C(0,s)$. The characteristic equation corresponding to the denominator of Eq. (19) matches that calculated from the eigenvalue approach in Eq. (14).

B. Integral Method Approximation (IMA)

Another way to convert the governing PDEs of a battery model to ODEs is to assume a distribution across the cell for the distributed variable of interest and integrate the governing equations to convert the PDE to a single ODE. In this section, the Integral Method Approximation (IMA) is applied to the benchmark problem. More information on the IMA can be found in [16], [18], [19], [20].

For the electrolyte diffusion problem with coupled domains described in Section I, the IMA assumes that the concentration has parabolic distributions in each domain

$$c(x,t) = \begin{cases} c_{0m}(t) + c_{1m}(t)x + c_{2m}(t)x^2 & \text{for } x \le L/2, \\ c_{0p}(t) + c_{1p}(t)x + c_{2p}(t)x^2 & \text{for } x \ge L/2. \end{cases} \tag{20}$$

The six coefficients in Eq. (20) can be solved from the two field equations ($x < L/2$ and $x > L/2$) and the four boundary conditions (3) and (4). Substitution ofb Eq. (20) into the Laplace Transform of Eq. (1) and integration yields

$$\begin{aligned} &\int_0^{L/2} \left(s\,\varepsilon_m C - D_m C'' - bI\right) dx \\ &= \frac{\varepsilon_m L}{2} s C_{0m} + \frac{\varepsilon_m L^2}{8} s C_{1m} + \left(\frac{\varepsilon_m L^3 s}{24} - L D_m\right) C_{2m} - \frac{bL}{2} I \\ &= 0 \end{aligned} \tag{21}$$

$$\begin{aligned} &\int_{L/2}^{L} \left(s\,\varepsilon_p C - D_p C'' + bI\right) dx \\ &= \frac{\varepsilon_p L}{2} s C_{0p} + \frac{3\,\varepsilon_p L^2}{8} s C_{1p} + \left(\frac{7\,\varepsilon_p L^3}{24} s - L D_p\right) C_{2p} + \frac{bL}{2} I \\ &= 0. \end{aligned} \tag{22}$$

Eqs. (3) give

$$C_{1m} = 0 \quad \text{and} \quad C_{1p} + 2LC_{2p} = 0. \tag{23}$$

Substitution of Eqs. (20) and (23) into the boundary conditions (4) yield

$$\begin{aligned} D_m C_{2m} + D_p C_{2p} &= 0, \\ C_{0m} + \frac{L^2}{4} C_{2m} - C_{0p} + \frac{3L^2}{4} C_{2p} &= 0. \end{aligned} \tag{24}$$

Solution of Eqs. (21) through (24) and substitution into the output equation

$$Y(s) = C(L,s) - C(0,s) = C_{0p} + C_{1p}L + C_{2p}L^2 - C_{0m} \tag{25}$$

gives the transfer function

$$\frac{Y(s)}{I(s)} = \frac{-3\,bL^2\,(\varepsilon_m + \varepsilon_p)\,(D_m + D_p)}{2\,\varepsilon_m\,\varepsilon_p L^2\,(D_m + D_p)\,s + 24\,D_m\,D_p\,(\varepsilon_m + \varepsilon_p)}. \tag{26}$$

The IMA can be extended to higher order approximations by evaluating the field equation at specific points in the domain. For each additional term in the approximation, an additional equation is added. In the coupled domain problem, for example, we can add $c_{3m}x^3$ to the approximation in Eq. (20) and solve the additional equation

$$\begin{aligned} &\varepsilon_m \left.\frac{\partial c}{\partial t}\right|_{x^*} - D_m \left.\frac{\partial^2 c}{\partial x^2}\right|_{x^*} - bI \\ &= \varepsilon_m \left(\dot{c}_{0m} + \dot{c}_{2m}{x^*}^2 + \dot{c}_{3m}{x^*}^3\right) - D_m\left(2c_{2m} + 3c_{3m}x^*\right) - bI \\ &= 0 \end{aligned} \tag{27}$$

where $x^* \in [0, L/2]$. Eq (27) is a first order differential equation, increasing the order of the approximation by one. Additional terms can be added to the approximation in Eq. (20) with additional equations from Eq. (27) evaluated at different x^*.

C. Padé Approximation Method (PAM)

The analytical solutions for battery cell related models can often be expressed in terms of transcendental transfer functions like Eq. (19). These transfer functions often involve hyperbolic functions that can also be written in terms of exponentials. The Padé Approximation works well for these infinitely differentiable functions that can be expanded in a power series at the origin [21], [22], [23], [24]. The N^{th} order Padé approximation of a transfer function $G(s)$ is a ratio of two polynomials in s where the denominator is of order N. For a proper transfer function, the numerator is of order N or less. The Padé Approximation Method can produce transfer functions with numerators of order 1 to N. The numerator order can be adjusted to obtain the best fit or the numerator order that provides the desired phase at high frequency can be used. The computational speed of the model depends strongly on the number of integrators in the model or the order of the denominator, and, to a lesser extent, the multiplications and additions associated with the numerator. In this paper, we focus only on model order as the computational cost metric so a high order numerator will probably provide the most accurate results.

We assume that the transfer function can be expanded in a power series at the origin as follows

$$G(s) = \sum_{k=0}^{2(N+1)} c_k \, s^k \tag{28}$$

where the coefficients c_k are calculated by repeated differentiation and evaluation of $G(s)$ at $s = 0$,

$$c_k = \left. \frac{d^k \, G(s)}{ds^k} \right|_{s=0}. \tag{29}$$

If $G(s)$ has a pole at the origin then we apply the power series expansion to $G^*(s) = s \, G(s)$ and substitute $G = P/s$ where P is the Padé approximation of G^*. The N^{th} order Padé approximation transfer function

$$P(s) = \frac{\sum_{m=0}^{N} b_m \, s^m}{1 + \sum_{n=1}^{N} a_n \, s^n} = \frac{num(s)}{den(s)}, \tag{30}$$

where we assume that the denominator and numerator both have order N. To determine $P(s)$ we must calculate the $N+1$ b_m and N a_m coefficients. The zeroth order term in the denominator is assumed to have a unity coefficient to normalize the solutions. The $2N+1$ linear equations that can be solved for the coefficients are determined from the polynomial equation

$$den(s) \sum_{k=0}^{2(N+1)} c_k s^k - num(s) = 0 \tag{31}$$

where the coefficients c_k are known from the power series expansion. Equation (31) produces a polynomial of order $2N(N+1)$ in s. The right hand side equals zero for all s so the coefficients of s must be zero. The first $N+1$ coefficients of s depend on both the unknown a_n and b_n coefficients. The remaining coefficients depend only on a_n. Thus, we set the coefficients of s^{N+2} to s^{2N+1} equal to zero to solve for $a_1, \ldots, a_N$. Then we substitute these solutions $a_1, \ldots, a_N$ into the coefficients of s^0 to s^N and set them equal to zero to solve for $b_0, \ldots, b_N$.

D. Ritz Method (RM)

The Ritz Method maintains the inherent symmetry of the operators in the governing PDEs. In battery systems, diffusion equations are symmetric, producing real eigenvalues and exponentially decaying response. The discretized **A** matrices generated by the Ritz method are also symmetric, ensuring real eigenvalues. The convergence properties of Ritz expansions have also been thoroughly studied. The eigenvalues converge monotonically from below, starting with negative eigenvalues that are smaller (larger in magnitude) and increase as the number of terms in the series increases. A Ritz approximation will never overpredict an eigenvalue.

The response is approximated by admissible functions that are continuous across the domain $0 \le x \le L$. A Fourier series solution is used with functions that satisfy the zero flux boundary conditions at $x = 0, L$. Starting with a weak form of the governing equation (1) that incorporates the natural (flux) boundary conditions. The requirement for continuous concentration at the interface of the two domains will be automatically satisfied by the continuity of the sinusoidal functions.

TABLE I
ELECTROLYTE DIFFUSION MODEL PARAMETERS

Parameter	Value
L	$100 \, \mu m$
t_0	0.363
A	$10,452 \, cm^2$
D^{ref}	$2.6 \times 10^{-6} \, cm^2/s$
ε_m	0.332
ε_p	0.28

E. Finite Element Method (FEM)

The Finite Element Method (FEM) is based on a weak form of the governing equation as was used in the Ritz Method. Rather than choosing functions that exist over the entire domain, however, FEM discretizes the domain $x \in [0, L]$ into $N-1$ subdomains or elements

$$\Omega_m = [(m-1)h, mh], \quad m = 1, 2, \ldots, N \tag{32}$$

In general, the length of each element can be varied to improve the accuracy in high flux regions and reduce the number of elements in regions with low gradients. For simplicity, we assume that the grid is uniform with each element having length h so $L = h(N-1)$. The concentrations at the endpoints of the domains are referred to as nodes $c_m(t) = c((m-1)h, t)$ for $m = 1, \ldots, N$. The N^{th} order FEM approximation has N nodes. FEM generates equations for the nodal dynamics that can be realized in state variable or transfer function forms. For more information and details on the FEM method, readers are referred to [15], [25].

F. Finite Difference Method (FDM)

The Finite Difference Method (FDM) is the simplest and most commonly used approach to the solution of the diffusion equations found in battery models. As with the finite element method, it easily handles spatially varying inputs and parameters. FDM can also be used on nonlinear problems. The method does not always maintain the symmetry of the underlying problem, however, and lacks the convergence guarantees of variational (FEM and Ritz) methods. Further information on this method can be found in [15], [16], [26].

III. MODEL RESPONSE

The response of a battery cell to step changes in charge/discharge current reveals how the concentration, potential, current density, and terminal voltage change with time under constant current loading. The parameters for the benchmark problem are shown in Table. I.

A. Time Response

The eigenvalues or poles of the analytical transfer function start at 0.14 rad/s, corresponding to a time constant of 7.1 seconds. The residues start at -1.05 and decrease with increasing frequency. The 26th residue is almost zero and the odd residues (1, 3, etc.) are generally several orders of magnitude smaller than the even residues.

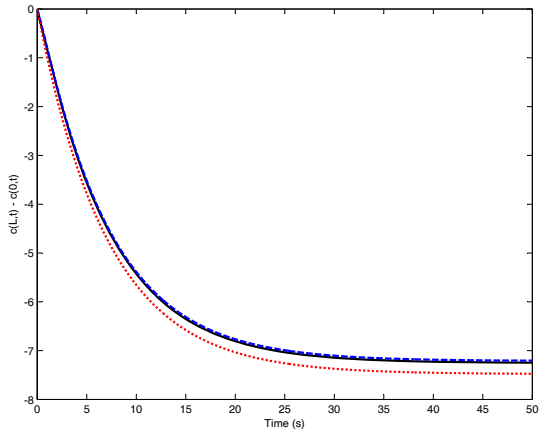

Fig. 2. Discharge step response for analytical solution with 26 (solid - black), 4 (dashed - blue) and 2 (dotted - red) term approximations: Output concentration $(c(L.t)-c(0.t))$

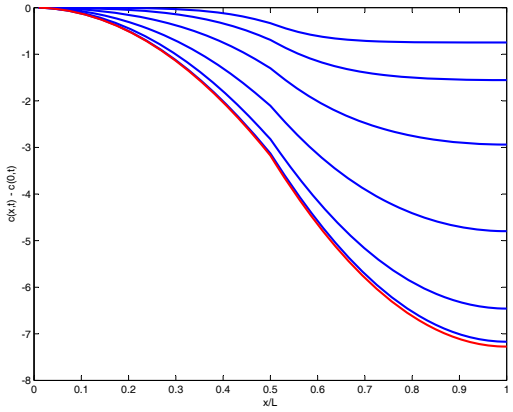

Fig. 3. Discharge step response for analytical solution with 26 term approximation: Concentration distribution $c(x,t)-c(0,t)$ (blue) at t = 1, 2, 4, 8, 16, 32 seconds and the steady state response (red).

The analytical discharge step response is shown in Fig. 2 for different truncation orders. The output is the difference in concentration across the cell $c(L,t)-c(0,t)$. The initial concentration is zero and current fluxes into the anode and fluxes out of the cathode, creating a negative change in relative concentration. The time response settles out in approximately five time constants (approximately 35 seconds) to the steady state value. As the model order increases from 2 to 4 to 26 modes, the response converges. Figure 3 shows the evolution of the concentration distribution with time. The concentration is initially zero across the cell. As time moves on the concentration in then anode increases and the cathode decreases. The results are plotted as differences in concentration relative to $c(0,t)$ so the distribution is always negative. It is clear that the zero flux boundary conditions are enforced at $x=0$ and $x=L$. At the junction between the two domains ($x=L/2$), the concentration and flux are continuous. The slope of the concentration distribution has a slight kink at $x=L/2$ associated with the change in diffusion coefficient.

B. Frequency Response

Figure 4 shows the analytical frequency response of the electrolyte diffusion model is calculated by substituting $s=$

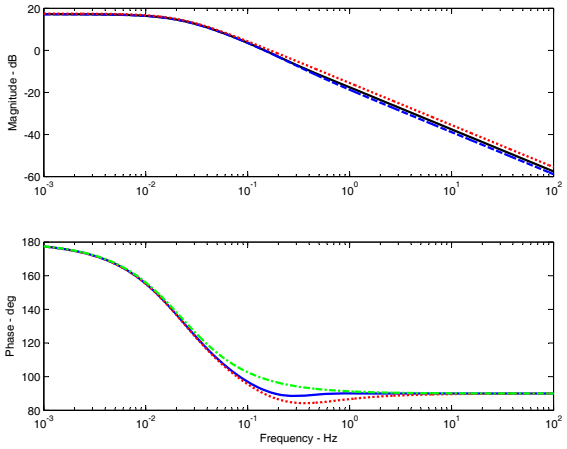

Fig. 4. Frequency response for exact solution (solid-black) and analytical solution with 26 (dashed - blue), 4 (dash-dotted - green) and 2 (dotted - red) term approximations: Output concentration $(C(L,i\omega)-C(0,i\omega))/I(i\omega)$.

TABLE II
APPROXIMATION ORDER REQUIRED FOR ELECTROLYTE DIFFUSION PROBLEM

Method	Step Response				Frequency Response			
	L_2		L_∞		L_2		L_∞	
	0.5%	1%	0.5%	1%	0.5%	1%	0.5%	1%
PAM	1	1	2	2	3	3	3	3
IMA	4	3	4	4	4	3	4	3
RM	6	4	6	4	6	4	6	4
AM	9	5	9	5	9	5	9	5
FEM	10	10	10	12	10	12	10	14
FDM	27	15	27	15	27	15	27	15

$i\omega$ into the transcendental transfer function Eq. (19) and calculating the associated gain and phase. The overall shape of the concentration frequency response is that of a low pass filter. The concentration has a steady state response at low frequency and rolls off at high frequency. The corner frequency is around 3×10^{-2} Hz. The exact solution is hidden behind the analytical solution truncated to 26 modes. The analytical solution converges as the number of terms in the truncated series increases from 2 to 4 to 26. Again, only a few modes are required to accurately capture the frequency response across the bandwidth of interest.

IV. MODELING COST, CONVERGENCE AND ACCURACY

To compare the convergence and accuracy of the various modeling methods, we introduce two error measurements that quantitatively compare the efficiency of the six methods using the L_2 norm and L_∞ norm. When calculating the accuracy, the 100th order analytical solution is adopted as the baseline model and the error is measured in both time domain and frequency domain.

Fig. 5 shows the errors versus truncation order, N, for the analytical method. All four error metrics approaches zero as the model order increases. The error metrics for the other discretization methods are summarized in Table II. The model order required to achieve 1% and 0.5% error are listed.

V. CONCLUSIONS

For all the methods, the error convergences as the model order increases. The Padé approximation method converges

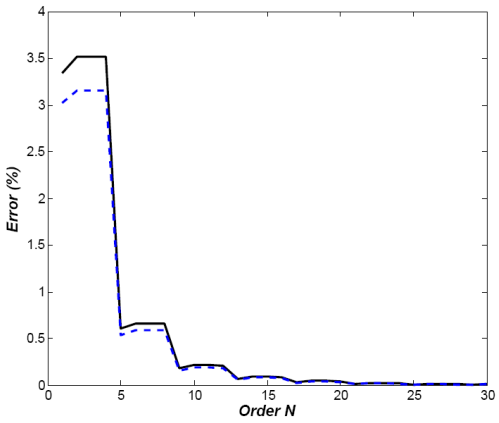

(a) Time domain

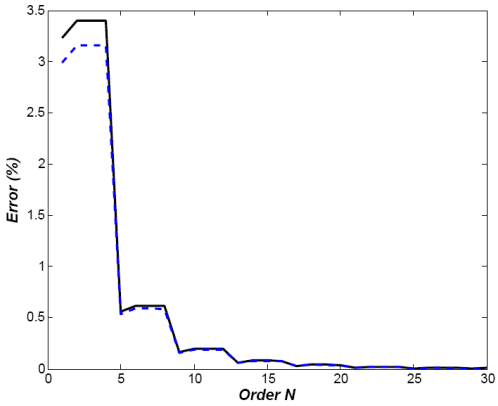

(b) Frequency domain

Fig. 5. Error metrics for analytical method solution, L_2 norm (solid - black) and L_∞ norm (dashed - blue)

the fastest. This method can only be applied to fairly simple problems where the power series can be determined analytically. The IMA and Ritz methods both use domain integration and provide the second and third best convergence. The Ritz method requires integration for all equations, complicating the process. As a variational method, however, the convergence is smooth and monotonic. The IMA equations are relatively easy to generate but the convergence characteristics are less well behaved. The analytical and FEM methods have similar convergence properties, coming in at fourth and fifth on the list. Both of these methods have guaranteed and smooth convergence properties. FDM is the least efficient method and lacks proven convergence properties but it is the easiest to formulate and solve. For the all of the methods the time and frequency domain L_2 and L_∞ error metrics are very close.

VI. ACKNOWLEDGMENTS

This work is supported by the Norfolk Southern Corporation and the Department of Energy.

REFERENCES

[1] J.Newman, *Electrochemical Systems*, 2nd ed. Englewood Cliffs, NJ: Prentice Hall, 1991.

[2] W. Gu and C. Wang, "Numerical modeling of the coupled electrochemical and transport processes in lead-acid batteries," *Journal of Power Sources*, vol. 144, no. 6, 1997.

[3] P. W. Appel, D. B. Edwards, and T. Stalick, "Modeling the effects of electrolyte diffusion and paste conductivity on lead/acid battery performance," *Journal of Power Sources*, vol. 46, no. 1, pp. 49 – 60, 1993.

[4] D. Fan and R. E. White, "A mathematical model of a sealed nickel-cadmium battery," *Journal of The Electrochemical Society*, vol. 138, no. 1, pp. 17–25, 1991.

[5] W. B. Gu, C. Y. Wang, and B. Y. Liaw, "The use of computer simulation in the evaluation of electric vehicle batteries," *Journal of Power Sources*, vol. 75, no. 1, pp. 151 – 161, 1998.

[6] P. D. Vidts, J. Delgado, and R. E. White, "Mathematical modeling for the discharge of a metal hydride electrode," *Journal of The Electrochemical Society*, vol. 142, no. 12, pp. 4006–4013, 1995.

[7] T. Fuller, M. Doyle, and J. Newman, "Simulation and optimization of the dual lithium ion insertion cell," *Journal of the Electrochemical Society*, vol. 141, pp. 1–10, 1994.

[8] K. Smith, C. Rahn, and C. Wang, "Control oriented 1d electrochemical model of lithium ion battery," *Energy Conversion and Management*, vol. 48, pp. 2565–2578, 2007.

[9] W. B. Gu and C. Y. Wang, "Thermal-electrochemical modeling of battery systems," *Journal of The Electrochemical Society*, vol. 147, no. 8, pp. 2910–2922, 2000.

[10] J. A. Prins-Jansen, J. D. Fehribach, K. Hemmes, and J. H. W. de Wit, "A three-phase homogeneous model for porous electrodes in molten-carbonate fuel cells," *Journal of The Electrochemical Society*, vol. 143, no. 5, pp. 1617–1628, 1996.

[11] P. P. Mukherjee, C.-Y. Wang, and Q. Kang, "Mesoscopic modeling of two-phase behavior and flooding phenomena in polymer electrolyte fuel cells," *Electrochimica Acta*, vol. 54, no. 27, pp. 6861 – 6875, 2009.

[12] M. Durr, A. Cruden, S. Gair, and J. McDonald, "Dynamic model of a lead acid battery for use in a domestic fuel cell system," *Journal of Power Sources*, vol. 161, 2006.

[13] Z. Salameh, M. Casacca, and W. Lynch, "A mathematical model for lead-acid batteries," *Energy Conversion, IEEE Transactions on*, vol. 7, no. 1, pp. 93 –98, mar. 1992.

[14] V. S. Arpaci, *Conduction Heat Transfer*. Reading, MA: Addison-Wesley Publishing Co., 1966.

[15] J. M. Hill and J. N. Dewynne, *Heat Conduction*. Oxford: Blackwell Scientific Publications, 1987.

[16] B. Gebhart, *Heat Conduction and Mass Diffusion*. New York, NY: McGraw-Hill, 1993.

[17] T. Jacobsen and K. West, "Diffusion impedance in planar, cylindrical, and spherical symmetry," *Electrochimica Acta*, vol. 40, no. 2, pp. 255 – 262, 1995.

[18] V. R. Subramanian, J. A. Ritter, and R. E. White, "Approximate solutions for galvanostatic discharge of spherical particles," *Journal of the Electrochemical Society*, vol. 148, no. 11, pp. E444–E449, 2001.

[19] V. R. Subramanian, D. Tapriyal, and R. E. White, "A boundary condition for porous electrodes," *Electrochemical and Solid-State Letters*, vol. 7, no. 9, pp. A259–A263, 2004.

[20] S. Santhanagopalan, Q. Guo, P. Ramadass, and R. E. White, "Review of models for predicting the cycling performance of lithium ion batteries," *Journal of Power Sources*, vol. 156, no. 2, pp. 620 – 628, 2006.

[21] G. A. Baker and P. Graves-Morris, *Pade Approximants*, 2nd ed., ser. Encyclopedia of Mathematics and Its Applications. Cambridge: Cambridge University Press, 1996, vol. 59.

[22] C. Brezinski and M. Redivo Zaglia, *Extrapolation Methods. Theory and Practice*. North Holland, 1991.

[23] G. H. Golub and C. F. Van Loan, *Matrix Computations*. Baltimore: Johns Hopkins University Press, 1989.

[24] J. S. Joel C. Forman, Saeid Bashash and H. Fathy, "Reduction of an electrochemistry-based li-ion battery health degradation model via constraint linearization and pad approximation," in *DSCC2010-4084*, Boston, MA, Sep 2010.

[25] J. N. Reddy and D. K. Gartling, *The finite element method in heat transfer and fluid dynamics*. Boca Raton, FL: CRC Press, Ltd., 2000.

[26] Y. Yener and S. Kakac, *Heat Conduction*. New York, NY: Taylor and Francis, 2008.